Detection of Quantum Phases via Out-of-Time-Order Correlators

Ceren B. Dağ, Kai Sun, and L.-M. Duan

Phys. Rev. Lett. **123**, 140602 — Published 4 October 2019

DOI: 10.1103/PhysRevLett.123.140602

Detection of quantum phases via out-of-time-order correlators

Ceren B. Dağ,[1,*] Kai Sun,[1] and L.-M. Duan[2]

[1] *Department of Physics, University of Michigan, Ann Arbor, Michigan 48109, USA*
[2] *Center for Quantum Information, IIIS, Tsinghua University, Beijing 100084, PR China.*

(Dated: September 13, 2019)

We elucidate the relation between out-of-time-order correlators (OTOCs) and quantum phase transitions via analytically studying the OTOC dynamics in degenerate spectrum. Our method points to key ingredients to dynamically detect quantum phases via out-of-time-order correlators for a wide range of quantum phase transitions and explains the existing numerical results in the literature. We apply our method to a critical model, XXZ model that numerically confirms our predictions.

Out-of-time-order correlators (OTOCs) [1] probe information scrambling in quantum systems of different nature [2–9] and reflect the symmetries [4, 7, 9] or lack thereof [2, 7, 10] of the underlying Hamiltonian. An OTOC, unlike a time-ordered four-point (or two-point) correlator [11], can determine the spatial and temporal correlations throughout the system, thus giving rise to a bound on information spread [9, 12, 13]. Through such bounds and the decay rate of an OTOC, one can dynamically detect thermal [7–9] and localized phases [4, 7, 9, 11, 14, 15]. Recently OTOC is numerically observed to be susceptible to also phase transitions either signaling criticality in a diverging Lyapunov exponent [16] or showing signatures of symmetry-broken phases in its saturation value [17]. The latter led to more research that shows the relation emerging in other forms, e.g. in excited states [18], or with more experimentally-relevant platforms and system parameters [19]. The interest in providing more verification for such an emergent relation is understandable, not only because the relation points to a practical potential for OTOC in dynamically probing quantum criticality, but also the relation is received as unexpected [17]. It is indeed an intriguing question how a chaos-detecting and out-of-time ordered correlator that is contributed by presumably all spectrum could also probe ground state physics. The reasons of this relation remains unknown as well as an answer to whether the relation is universal. Motivated by these questions, here, we develop a method on OTOC dynamics to obtain intuition for the emerging relation between quantum phase transitions and out-of-time-order correlators. Remarkably it is possible to dynamically decompose OTOC and show that the ground state physics is the leading order contribution to it under the criteria that our method provides. This is the origin why OTOC saturation value could detect the ground state degeneracy. Therefore, we reach to the conclusion that the OTOC is susceptible to long-range order, while the quasi-long range order is not visible to it. Our method provides additional insights regarding the relation, e.g. (i) the relation is not restricted to already-studied models and 1D [17, 19]; (ii) the relation can be extended to include the phase transitions in other eigenstates [18]. Hence, our theory elucidates the reasons of this *unexpected* connection, renders it intuitive and universal with further insights. To verify our method, we study the dynamics of 1D critical XXZ chain, where there are Ising and critical XY phases.

Method. Our aim is to be able to come up with an expression that predicts the saturation value of OTOC for long times in the spirit of Eigenstate Thermalization Hypothesis (ETH) [20, 21]. The out-of-time-order correlation function can be defined as

$$F(t) = \left\langle W^\dagger(t) V^\dagger W(t) V \right\rangle, \tag{1}$$

where V and W are local operators and the expectation value is over an initial state $|\psi(0)\rangle$. This initial state could be chosen as the ground state [6, 17], or a random Haar-distributed state [9, 12] to approximate an equiprobable state $\mathcal{I}$ in Eq. (1) [22–24]. Eventually, the original definition that is the commutator growth $-\mathrm{Tr}\left(\frac{\exp[-\beta H]}{Z}\left[W(t), V\right]^2\right)$ [10] could be re-expressed in terms of the OTOC of operators W and V with an initial state at the inverse temperature β. Therefore we can probe the information scrambling through OTOCs [6, 8, 9, 25, 26].

Given $|\psi(t)\rangle = \sum_\alpha c_\alpha e^{-iE_\alpha t}|\psi_\alpha\rangle$, where $|\psi_\alpha\rangle$ are eigenstates of the Hamiltonian with the associated eigenvalues E_α, we define a modified initial state $|\psi'(0)\rangle = V|\psi(0)\rangle$ and have $|\psi'(t)\rangle = \sum_\beta b_\beta e^{-iE_\beta t}|\psi_\beta\rangle$. Then the OTOC, Eq. (1), can be recast to a fidelity measure of 3-point function, and with the help of completeness relation $\sum_\gamma |\psi_\gamma\rangle\langle\psi_\gamma| = \mathbb{I}$ becomes

$$F(t) = \sum_{\alpha,\beta,\gamma,\gamma'} c_\alpha^* b_\beta e^{-i(E_\beta - E_\alpha + E_\gamma - E_{\gamma'})t} W^\dagger_{\alpha\gamma} V^\dagger_{\gamma\gamma'} W_{\gamma'\beta},$$

where $\langle\psi_\alpha| W |\psi_\gamma\rangle = W_{\alpha\gamma}$ are EEVs (eigenstate expectation values) [27]. Now one can derive the saturation value for long times as well as dynamical features, such as revival timescales in integrable Hamiltonians [28].

We study the saturation value in long times, since this value is expected to contain the signature of quantum phases. For long enough times, equilibration in OTOC dynamics can be obtained only when the phase decoheres. Then the equilibration value can be obtained

by requesting $E_\beta - E_\alpha + E_\gamma - E_{\gamma'} = 0$. This condition can be satisfied with four different scenarios: (i) $E_\alpha = E_\beta$ and $E_\gamma = E_{\gamma'}$; (ii) $E_\alpha = E_\gamma$ and $E_\beta = E_{\gamma'}$; (iii) $E_\alpha = E_\beta = E_\gamma = E_{\gamma'}$, which is contained both in (i) and (ii); (iv) $E_\beta - E_\alpha + E_\gamma - E_{\gamma'} = 0$ with $E_\beta \neq E_\alpha \neq E_\gamma \neq E_{\gamma'}$. If a non-degenerate spectrum is assumed, i.e. $E_\alpha = E_\beta$ implies $\alpha = \beta$, the OTOC reduces to,

$$F_{t\to\infty} = \sum_{\alpha,\gamma} c_\alpha^* b_\alpha |W_{\alpha\gamma}|^2 V_{\gamma\gamma}^\dagger + \sum_{\alpha,\beta} c_\alpha^* b_\beta W_{\alpha\alpha}^\dagger V_{\alpha\beta}^\dagger W_{\beta\beta} \quad (2)$$
$$- \sum_{\alpha} c_\alpha^* b_\alpha |W_{\alpha\alpha}|^2 V_{\alpha\alpha}^\dagger + \sum_{\alpha\neq\beta\neq\gamma\neq\gamma'} c_\alpha^* b_\beta W_{\alpha\gamma}^\dagger V_{\gamma\gamma'}^\dagger W_{\gamma'\beta},$$

with four terms corresponding to four conditions (i)-(iv), respectively. We note that writing OTOC as in Eq. 2 proved to be useful previously to understand the quantum chaotic systems better, e.g. in chaotic spin chains with conserved quantities that also obey ETH, decay to zero is not supposed to be exponential, but inverse polynomial in system size [29] and OTOCs capture eigenstate correlations that ETH cannot [30]. These correlations can readily be seen in the first, second and the fourth terms of Eq. 2. See Supplement S5 [24] for some remarks that immediately follow from Eq. 2 about systems with non-degenerate chaotic spectra. Now we are going to generalize Eq. (2) to a more generic form, which allows degeneracy in the energy spectra, because a quantum phase transition usually involves energy degeneracy, e.g. degeneracy from spontaneous symmetry breaking or other sources [31]. We group all eigenstates of the Hamiltonian into degenerate sets labeled by θ, and each state in its corresponding set is denoted by α for an eigenstate $\psi_{[\theta,\alpha]}$. The OTOC can be reorganized with the new notation, which is one main result of this Letter,

$$F(t\to\infty) = \sum_{\theta\theta'} \sum_{\alpha\beta\gamma\gamma'} c_{[\theta,\alpha]}^* \left(b_{[\theta,\beta]} W_{[\theta,\alpha][\theta',\gamma]}^\dagger V_{[\theta',\gamma][\theta',\gamma']}^\dagger W_{[\theta',\gamma'][\theta,\beta]} + b_{[\theta',\beta]} W_{[\theta,\alpha][\theta,\gamma]}^\dagger V_{[\theta,\gamma][\theta',\gamma']}^\dagger W_{[\theta',\gamma'][\theta',\beta]} \right) \quad (3)$$
$$+ \sum_{\alpha\beta\gamma\gamma'} \left(- \sum_{\theta} c_{[\theta,\alpha]}^* b_{[\theta,\beta]} W_{[\theta,\alpha][\theta,\gamma]}^\dagger V_{[\theta,\gamma][\theta,\gamma']}^\dagger W_{[\theta,\gamma'][\theta,\beta]} + \sum_{\theta\neq\theta'\neq\phi\neq\phi'} c_{[\theta,\alpha]}^* b_{[\theta',\beta]} W_{[\theta,\alpha][\phi,\gamma]}^\dagger V_{[\phi,\gamma][\phi',\gamma']}^\dagger W_{[\phi',\gamma'][\theta',\beta]} \right).$$

Here, $\theta, \theta', \phi, \phi'$ denote degenerate sets while $\alpha, \beta, \gamma, \gamma'$ denote quantum states in their corresponding sets. Eq. (3) can predict the saturation value of OTOC accurately if the OTOC saturates at a finite time. If the OTOC does not saturate or shows transient effects, Eq. (3) still predicts the time-average of OTOC signal $\bar{F} = 1/\mathcal{T} \int dt F(t)$ over a time interval $\mathcal{T}$ with sufficient accuracy. In this sense, Eq. (3) is not limited to long-time dynamics $t \to \infty$ [24].

We look for the criteria that the ground state subspace contribution is leading order in the OTOC saturation value Eq. (3). For this, we first set $W = V$ as the order parameter operator in Eq. (3) for convenience. Then we expand the coefficients $b_{[\theta,\beta]} = \sum_{\kappa,\tau} W_{[\theta,\beta][\kappa,\tau]} c_{[\kappa,\tau]}$ in Eq. (3) by using the initial state. If (i) the initial state is set to the state where the phase transition is expected to happen, e.g. the ground state(s) $c_{[1,1]} = 1$; and (ii) we apply an ansatz on the matrix elements of the operator projected on this state, e.g. $|W_{[1,\alpha][\theta,\beta]}|^2 \ll 1$, where $\theta \neq 1$ is a different energy subspace than the subspace of the ground state(s), we observe the following dynamical decomposition:

$$F(t\to\infty) = F_{\rm gs}(t\to\infty) + F_{\rm ex}(t\to\infty). \quad (4)$$

Here $F_{\rm gs}(t\to\infty)$ is the ground subspace contribution, whereas the $F_{\rm ex}(t\to\infty)$ is the contribution of higher energy excitations. The latter is a correction to the ground-state physics in the OTOC, when the criteria are satisfied. The assumption on the initial state sets the scrambling discussed in the rest of the paper to effectively zero temperature. Whereas the operator ansatz becomes even more specific for the phase of interest. If there is a symmetry-broken long-range order to capture, the fluctuations between the matrix elements of the operator are suppressed in the ground state subspace, meaning there is at least a pair of matrix elements accumulating the order $\to |W_{[1,\alpha][1,\beta]}|^2 \sim \mathcal{O}(1)$. This modifies the operator ansatz as $|W_{[1,\alpha][1,\beta]}|^2 \gg |W_{[1,\gamma][\theta,\gamma']}|^2$ for the ordered phase. Thus, we derive the expression for $F_{\rm gs}(t\to\infty)$ in the ordered phase as,

$$F_{\rm gs}(t\to\infty) \sim \quad (5)$$
$$\sum_{\beta,\gamma,\gamma'} W_{[1,1][1,\gamma]} W_{[1,\gamma][1,\gamma']} W_{[1,\gamma'][1,\beta]} W_{[1,\beta][1,1]},$$

while the operator ansatz simultaneously implies that the OTOC is dominated by the ground state physics, $F_{\rm gs} \gg F_{\rm ex}$ in the ordered phase. On the other hand, the fluctuations between the matrix elements of the operator are maximal in a disordered phase, implying $W_{[1,\alpha][1,\beta]} \sim 0$ for all in the ground state subspace which results in $F_{\rm gs}(t\to\infty) \sim 0$. Therefore, the OTOC is dominated by the correction terms that are contributed by the excitations in the spectrum $F_{\rm ex}(t\to\infty)$. This result is an important insight that originates from the dynamical decomposition method and cannot be observed only

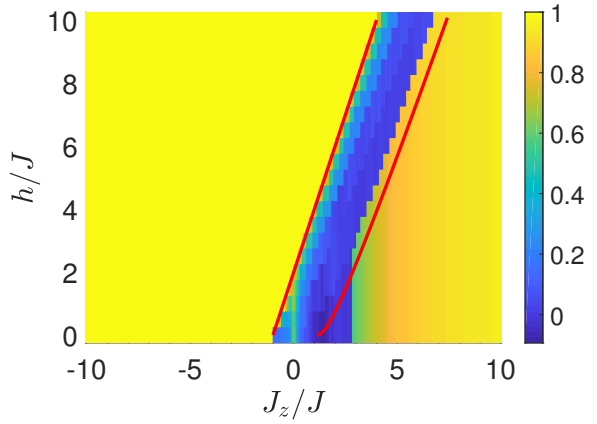

FIG. 1. Phase diagram based on the OTOC saturation values via Eq. (3), x-axis is the spin interaction strength in the z-direction J_z and y-axis is the magnetic field h, for $N = 14$ system size and σ_i^z bulk spin operator, when periodic boundary conditions are set and the initial state is a ground state. The red lines are the phase boundaries based on Bethe ansatz technique for infinite-size system [32].

via real-time dynamics simulations, e.g. in Ref. [17]. In addition, the operator ansatz $|W_{[1,\alpha][\theta,\beta]}| \ll 1$ guarantees a bounded correction term $F_{\text{ex}}(t \to \infty) \ll 1$. As a result, (i) the OTOC is able to capture the degeneracy in the ground state (Eq. (5)) and, (ii) the correction of the excited states always remains bounded; all of which explains why the OTOC differentiates an ordered phase from a disordered one, e.g. in ground state [17] or excited-state [18] phase transitions. A mixed initial state (e.g. finite or infinite temperature) violates the initial state assumption, hence suggesting a smoothed phase boundary by washing away the sharp signature at the transition point [19]. Hence the dynamical decomposition method reveals the key ingredients of the emergent relation between information scrambling and symmetry-breaking phase transitions, rendering this unexpected numerical observation [17] a fundamental connection.

Advanced numerical methods (Lanczos, tensor networks) can be employed to determine only the lowest-lying states to give the leading order term in OTOC, Eq. (5). In this sense, Eq. (5) provides us a low-cost alternative to simulating the real-time OTOC dynamics in the computation of the OTOC saturation value when we use the OTOC to probe criticality. Finally, we predict that the ground state contribution to the OTOC saturation cannot efficiently distinguish quasi-long range order from a disordered phase. Because, the quasi-long range order produces zero expectation value for the order parameter (per site): $W_{[1,\alpha][1,\beta]} \sim 0$, similar to a disordered phase, and hence $F_{\text{gs}}(t \to \infty) \sim 0$ follows with correction term dominating the OTOC saturation $F(t \to \infty)$. In the following we will provide verification for our method and theory on the 1D XXZ model.

Model and results. The Hamiltonian of the XXZ model reads,

$$H = J \sum_i \left(\sigma_i^x \sigma_{i+1}^x + \sigma_i^y \sigma_{i+1}^y + \frac{J_z}{J} \sigma_i^z \sigma_{i+1}^z \right) + h \sum_i \sigma_i^z,$$

where σ_i^n are spin-1/2 Pauli matrices with energy scale set to J and hence time scale set to $1/J$; J_z/J and h are the z-axis spin coupling strength and the magnetic field strength, respectively. The red lines in Fig. 1 show the phase boundaries produced by an exact method (Bethe Ansatz) for an infinite-size system. Therefore, this model has three phases: two gapped Ising phases (ferromagnetic and antiferromagnetic) at large $|J_z/J|$ and a gapless XY phase with quasi-long range order for small $|J_z/J|$, i.e. the Berezinskii-Kosterlitz-Thouless transition [33, 34]. We choose the OTOC operators as σ_i^z or σ_i^x for the spin at the ith site, based on the order parameters of the ferromagnetic Ising phase ($\sum_i \sigma_i^z$), antiferromagnetic Ising phase ($\sum_i (-1)^i \sigma_i^z$), and the XY-phase ($\sum_i \sigma_i^x$). Fig. 1 shows the phase diagram based on the saturation values of OTOCs with σ_i^z [computed using Eq. (3) for a system of $N = 14$ spins]. We numerically confirm our theory with OTOC saturation values that are either nonzero or nearly zero in the Ising and XY phases. In fact, the OTOC recovers the phase boundaries of the Bethe ansatz solution: the agreement is perfect at the ferromagnetic-XY phase boundary and approximate at the antiferromagnetic-XY boundary due to significant finite-size effects [24].

We plot two cross-sections from Fig. 1 in Fig. 2a where the lines with orange-squares ($h/J = 0$) and blue-circles ($h/J = 4$) are the saturation values, Eq. (3) for a short-time $tJ \sim \frac{\pi}{4} 10^1$ (long-time results in [24]). We also plot the leading order term in the saturation, $F_{\text{gs}}(t \to \infty)$ in Fig. 2a with purple-cross ($h/J = 0$) and red-diamond ($h/J = 4$) lines. The OTOC saturation exactly reduces to the ground state contribution with no correction $F_{\text{ex}} = 0$ in the Ising-ferromagnet, meaning that the saturation value in the ordered phase is exactly predicted by the Eq. (5). The reason follows as: the spins are fully polarized in the ferromagnetic ground states, and they belong to the opposite magnetization sectors of the Hamiltonian which has magnetization conservation $[H, S_z] = 0$ ($S_z = \sum_i \sigma_i^z$). Since they are the only states of their corresponding magnetization sectors, the fluctuations in the matrix elements are exactly zero, $|W_{[1,\alpha][\theta,\beta]}| = 0$. This is why the system does not scramble information at all $F(t \to \infty) = 1$, even though the XXZ model is an interacting model. We emphasize that this non-scrambling is not due to integrability of XXZ model, rather it is the signature of critical order. The rotational symmetry also protects the ferromagnetic ground states from hybridizing, all of which results in no finite-size effects at the phase boundary from ferromagnet to XY-paramagnet. In the disordered-XY phase ($h/J = 0$), the ground state contribution is zero $F_{\text{gs}} = 0$, leaving the

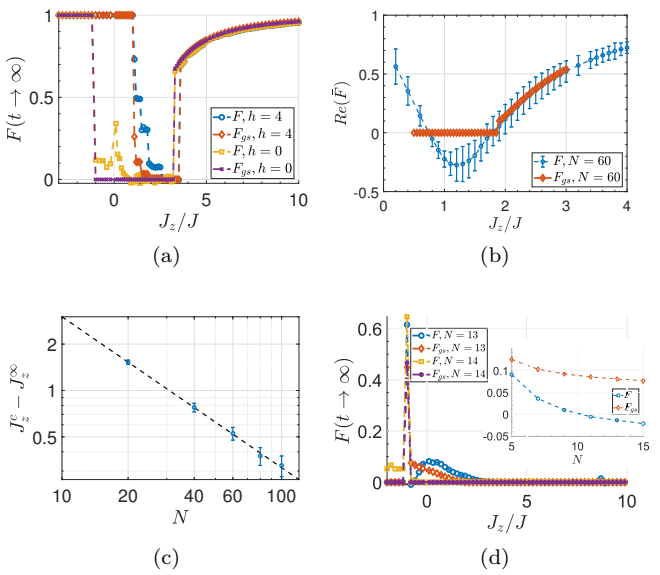

FIG. 2. (a) The OTOC saturation values for a periodic-boundary chain with $N = 14$ size and a short-time of $tJ = \frac{\pi}{4}10^1$ at fields $h/J = 0$ (orange-squares: Eq. (3), purple-crosses: Eq. (5)) and $h/J = 4$ (blue-circles: Eq. (3), red-diamonds: Eq. (5)), for σ_i^z operator. (b) Real-time dynamics (blue-circles) averaged over a time interval $tJ = 10$, $\bar{F}$, and its ground state contribution F_{gs} (orange-diamonds) with DMRG algorithm and MPS for $N = 60$ at $h/J = 0$. (c) System size scaling of F_{gs} shows $J_z^c = aN^\xi + J_z^\infty$ with exponent $\xi = -0.98$ and $J_z^\infty = 1.02$. (d) The OTOC saturation values for σ_i^x operator at $h/J = 0$, $N = 13$ (blue-circles: Eq. (3), red-diamonds: Eq. (5)) and $N = 14$ (orange-squares: Eq. (3), purple-crosses: Eq. (5)) for time $tJ = \frac{\pi}{4}10^3$. Inset: System-size scaling of Eq. (3) (blue-circles) and Eq. (5) (red-diamonds) at $J_z/J = -0.9$.

correction term to dominate the saturation value, however with a small magnitude as explained above. This is the reason of mismatch between the OTOC saturation value and its leading order term, seen in the XY-phase of Fig. 2a, while we are still able to differentiate the disordered phase from the ordered phases. Finally, in the Ising-antiferromagnet the exact agreement between Eqs. (3) and (5) takes place only at the $J_z/J \to \infty$ limit. As we approach the phase boundary to XY-phase, the fluctuations between matrix elements gradually increase, $|W_{[1,\alpha][1,\beta]}| \to 0$ [24], result in a nonzero but small correction term to the ground-state contribution and eventually drive the phase transition. Since the finite-size effect is significant for small sizes with exact methods, we apply density-matrix renormalization group (DMRG) algorithm with matrix product states (MPS) [24, 35] to a system with $N = 60$ and compute the real-time dynamics averaged over a short-time interval of $tJ = 10$ shown with blue-circles in Fig. 2b with orange-diamonds being F_{gs}, Eq. (5). Note that the transition point significantly shifts towards the equilibrium phase transition point, $J_z/J = 1$. We extract the system-size scaling parameters from our DMRG computations, Fig. 2c and observe that the system indeed approaches to the equilibrium transition point when $N \to \infty$, $J_z^c = aN^\xi + J_z^\infty$ with exponent $\xi = -0.98$ and $J_z^\infty = 1.02$ with a power-law scaling.

We plot the OTOC with σ_i^x operator for $N = 13$ (blue-circles) in Fig. 2d: the OTOC saturation remains small in all three phases and thus the OTOC can hardly distinguish the XY-ordered from XY-disordered phases. When the chains with even number of spins are used ($N = 14$, orange-squares) in the theory, we do not even obtain any difference between the phases. This is in agreement with our theoretical predictions discussed previously. Additionally, the fluctuations between the matrix elements of quasi-long range order parameter σ_i^x are always maximal regardless of the phase. Hence, we observe the mismatch between the OTOC saturation and its ground state contribution (red-diamonds $N = 13$ and purple crosses $N = 14$). The inset of Fig. 2d shows that the OTOC saturation value and its ground state contribution, both, decrease with the system size for odd-numbered chains, exhibiting that the OTOC saturation cannot capture the quasi-long range order in bigger systems and thermodynamic limit. We briefly note that the detection of the order at $J_z/J = -1$ is robust due to the massive degeneracy in the ground state at this point of different symmetry (SU(2) symmetry).

Conclusion. Our theoretical predictions on the XXZ model can be experimented with cold atoms [36]. Based on the studies in literature [17–19] and our results in the XXZ model, our method seems to be universal in explaining the reasoning behind the relation between scrambling and the quantum criticality. In this sense, our method is an analogue of Eigenstate Thermalization Hypothesis: It tells us the criteria of how scrambling probes criticality; though it is independent of the integrability of the system, unlike ETH. Dynamical decomposition of OTOC is a complementary tool to the real-time evolution of a state in determining the OTOC saturation value. However in addition to providing the saturation value, it also presents us the conditions for OTOC to show either order or disorder. Based on this fact, the leading order term in our theory, Eq. (5), could mark the phase transition points via system-size scalings. In conclusion, given that the initial state of OTOC is a state where the phase transition is expected to happen and the off-diagonal matrix elements of the operator are sufficiently suppressed in this state (or degenerate state subspace), OTOC could be used to dynamically detect the quantum phases with long-range order and capture the symmetry-breaking quantum phase transitions.

Acknowledgements. C.B.D. thanks P. Myles Eugenio for interesting discussions and comments on the manuscript.

* cbdag@umich.edu

[1] A. I. Larkin and Y. N. Ovchinnikov, Soviet Journal of Experimental and Theoretical Physics **28**, 1200 (1969).
[2] Y. Sekino and L. Susskind, Journal of High Energy Physics **10**, 065 (2008), arXiv:0808.2096 [hep-th].
[3] N. Lashkari, D. Stanford, M. Hastings, T. Osborne, and P. Hayden, Journal of High Energy Physics **4**, 22 (2013), arXiv:1111.6580 [hep-th].
[4] B. Swingle and D. Chowdhury, Phys. Rev. B **95**, 060201 (2017), arXiv:1608.03280 [cond-mat.str-el].
[5] K. Hashimoto, K. Murata, and R. Yoshii, Journal of High Energy Physics **10**, 138 (2017), arXiv:1703.09435 [hep-th].
[6] M. Grttner, J. Bohnet, A. Safavi-Naini, M. L. Wall, J. J. Bollinger, and A. Rey, *Nature Physics*, **13** (2016).
[7] X. Chen, T. Zhou, D. A. Huse, and E. Fradkin, Annalen der Physik **529**, 1600332.
[8] A. Bohrdt, C. B. Mendl, M. Endres, and M. Knap, New Journal of Physics **19**, 063001 (2017), arXiv:1612.02434 [cond-mat.quant-gas].
[9] C. B. Dağ and L. M. Duan, Phys. Rev. A **99**, 052322 (2019), arXiv:1807.11085 [quant-ph].
[10] J. Maldacena, S. H. Shenker, and D. Stanford, Journal of High Energy Physics **2016**, 106 (2016).
[11] Y. Huang, Y.-L. Zhang, and X. Chen, Annalen der Physik **529**, 1600318.
[12] D. J. Luitz and Y. Bar Lev, Phys. Rev. B **96**, 020406 (2017).
[13] S. Xu and B. Swingle, arXiv e-prints , arXiv:1802.00801 (2018), arXiv:1802.00801 [quant-ph].
[14] R. Fan, P. Zhang, H. Shen, and H. Zhai, ArXiv e-prints (2016), arXiv:1608.01914 [cond-mat.quant-gas].
[15] R.-Q. He and Z.-Y. Lu, Physical Review B **95**, 054201 (2017), arXiv:1608.03586 [cond-mat.dis-nn].
[16] H. Shen, P. Zhang, R. Fan, and H. Zhai, Phys. Rev. B **96**, 054503 (2017), arXiv:1608.02438 [cond-mat.quant-gas].
[17] M. Heyl, F. Pollmann, and B. Dóra, Phys. Rev. Lett. **121**, 016801 (2018).
[18] Q. Wang and F. Pérez-Bernal, arXiv e-prints , arXiv:1812.01920 (2018), arXiv:1812.01920 [quant-ph].
[19] Z.-H. Sun, J.-Q. Cai, Q.-C. Tang, Y. Hu, and H. Fan, arXiv e-prints , arXiv:1811.11191 (2018), arXiv:1811.11191 [quant-ph].
[20] M. Srednicki, Journal of Physics A Mathematical General **32**, 1163 (1999), cond-mat/9809360.
[21] M. Srednicki, in *eprint arXiv:chao-dyn/9511001* (1995).
[22] S. Sugiura and A. Shimizu, Phys. Rev. Lett. **108**, 240401 (2012).
[23] D. J. Luitz and Y. B. Lev, Annalen der Physik **529**, 1600350 (2017), arXiv:1610.08993 [cond-mat.dis-nn].
[24] See Supplemental Material [url] for additional computations, which includes Refs. [37–42].
[25] J. Li, R. Fan, H. Wang, B. Ye, B. Zeng, H. Zhai, X. Peng, and J. Du, Physical Review X **7**, 031011 (2017), arXiv:1609.01246 [cond-mat.str-el].
[26] B. Swingle, G. Bentsen, M. Schleier-Smith, and P. Hayden, Phys. Rev. A **94**, 040302 (2016).
[27] M. Rigol, V. Dunjko, and M. Olshanii, Nature (London) **452**, 854 (2008), arXiv:0708.1324 [cond-mat.stat-mech].
[28] C. B. Dağ, S.-T. Wang, and L.-M. Duan, Phys. Rev. A **97**, 023603 (2018).
[29] Y. Huang, F. G. S. L. Brandão, and Y.-L. Zhang, Phys. Rev. Lett. **123**, 010601 (2019).
[30] A. Chan, A. De Luca, and J. T. Chalker, Phys. Rev. Lett. **122**, 220601 (2019).
[31] C. B. Dağ, L. M. Duan, and K. Sun, arXiv e-prints , arXiv:1906.05241 (2019), arXiv:1906.05241 [quant-ph].
[32] F. Franchini, ed., *Lecture Notes in Physics, Berlin Springer Verlag*, Lecture Notes in Physics, Berlin Springer Verlag, Vol. 940 (2017) arXiv:1609.02100 [cond-mat.stat-mech].
[33] V. L. Berezinskiĭ, Soviet Journal of Experimental and Theoretical Physics **32**, 493 (1971).
[34] J. M. Kosterlitz and D. J. Thouless, Journal of Physics C Solid State Physics **5**, L124 (1972).
[35] ITensor Library (version 2.0.11) http://itensor.org.
[36] L.-M. Duan, E. Demler, and M. D. Lukin, Phys. Rev. Lett. **91**, 090402 (2003).
[37] G. Biroli, C. Kollath, and A. M. Läuchli, Phys. Rev. Lett. **105**, 250401 (2010).
[38] P. Hayden, D. W. Leung, and A. Winter, Communications in Mathematical Physics **265**, 95 (2006), arXiv:quant-ph/0407049 [quant-ph].
[39] S. Goldstein, J. L. Lebowitz, R. Tumulka, and N. Zanghì, Phys. Rev. Lett. **96**, 050403 (2006).
[40] S. Popescu, A. J. Short, and A. Winter, Nature Physics **2**, 754 (2006).
[41] P. Reimann, Phys. Rev. Lett. **99**, 160404 (2007).
[42] M. P. Zaletel, R. S. K. Mong, C. Karrasch, J. E. Moore, and F. Pollmann, Phys. Rev. B **91**, 165112 (2015).